A machine for conics and oblique trajectories

Pietro Milici, Frédérique Plantevin, Massimo Salvi

A machine for conics and oblique trajectories

Pietro Milici, Frédérique Plantevin, Massimo Salvi

Abstract

In his 1637 *Géométrie* Descartes introduced a general method to adopt algebra in geometrical problem solving. Such a method was still based on geometric constructions, and curves were introduced as traces of ideal machines. Differently from Descartes' idea of limiting geometry to algebraic curves, in the second half of the 17th century, mathematicians looked for an appropriate geometrical legitimation to introduce non-algebraic curves. A general problem that originated a wide class of transcendental curves was the inverse tangent problem: new curves were introduced given the properties that their tangents have to satisfy. Suitable ideal and also real machines have been designed and realized to solve this class of problems.

The aim of this paper is to propose an original machine that, by the solution of inverse tangent problems, traces both conics and some transcendental curves obtained as oblique trajectories of confocal conics. For such a machine we also provide the 3D printable model: in this way we wish to allow a widespread of this kind of machines between mathematical enthusiasts but also for laboratory activities in teaching mathematics.

1 Introduction

In his 1637 *Géométrie* Descartes introduced a general method to adopt polynomial algebra in order to solve geometrical problems. We have to keep in mind that Cartesian method was still based on geometric constructions, and curves were accepted when continuously traced by ideal machines (exactness problem), as highlighted in [5]. However, although the French philosopher gave some examples, the *Géométrie* did not provide a well-defined class of machines for algebraic constructions. A general theory for such constructions can be considered that of linkages, considered as fixed-length rods jointed each other: the main result, the so-called "universality theorem" (proved in [12] even though with some flaws), states that any bounded part of a planar algebraic curve can be traced by a linkage (if we do not consider intersection problems due to physical rods).

Descartes' foundation limited geometry to algebraic curves: however, already in the second half of the 17th century, this boundary has no longer been widely accepted by mathematicians, who looked for an appropriate geometrical legitimation to introduce non-algebraic curves. Between other less powerful geometrical methods, a general problem that originated a wide class of transcen-

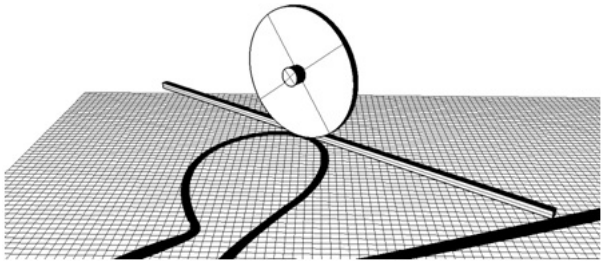

Figure 1: Considering a wheel rolling on a curve, the direction of the wheel (in the image represented by a bar) is the tangent to the curve.

dental curves was the *inverse tangent problem* (in a modern setting, it is found in the geometrical solution of differential equations). While the direct tangent problem, i.e. to find an object tangent to a given curve while satisfying certain properties, had been present at least since classical Greek geometry, it was only after Descartes that mathematicians tried to consider new curves given the properties that their tangents have to satisfy. The first documented appearance of an inverse tangent problem is attributed to the architect Claude Perrault in the late 17th century: a new curve, the tractrix, has been introduced as the trace of a pocket watch on a plane while moving the endpoint of its chain along a straight line. The role of traction in the first instrumental ways of generating a curve given its tangent conditions made such constructions termed "tractional:" these constructions interested many important mathematicians mainly from the end of the 17th to the first half of the 18th century, from Leibniz to Euler (see [4], [27] or also, for a brief introduction, [6]).

Physically, the component solving an inverse tangent problem had to avoid the lateral motion of a point with respect to a given direction. Instead of using a chain watch, this can be better accomplished by something that, like the blade of a pizza-cutter or the front wheel of a bike, guides the direction of the motion (cf. Figure 1).

Specifically, while machines in the *Géométrie* pose only "position constraints," i.e., according to mechanics, *holonomic* constraints (they pose relations between the position variables without any reference to the speed or the direction of the motion), tractional motion also poses "direction constraints" that analytically involve the derivatives, thus are *non-holonomic* . The constructive boundaries of tractional machines (i.e. linkages extended by wheels, firstly introduced in [17]) appeared only recently in [19] as a differential extension of Kempe's universality theorem. In this new setting, the language of polynomial algebra is extended by differential algebra, and the limit of constructions is no longer given by curves but by functions: the class of functions generable by tractional machines coincides with the algebraic differential functions, i.e. solutions of non-trivial polynomials $P(t, x(t), x'(t), \ldots, x^{(n)}(t)) = 0$.

Tractional machines recently found a new interest not only in foundations

but also in didactical laboratory activities (see [16]) because such machines allow constructing curves by the geometrical resolution of differential equations.

The aim of this paper is to propose an original machine (invented by the corresponding author) that, by the solution of inverse tangent problems, traces both conics and some transcendental curves obtained as oblique trajectories of confocal conics. For such a machine we also provide the 3D printable model: in this way we wish to allow a widespread of this kind of machines between mathematical enthusiasts but also for laboratory activities in teaching mathematics.

2 Machines for conic sections

Machines to construct curves were historically relevant in geometry not only for practical/artistic aims but also for foundational/theoretical purposes (e.g. the "exactness problem of geometric constructions" of Descartes [5] or Leibniz [3] in the early modern period). Specifically, we can note that the same curves can be traced by very different devices, each one physically implementing a geometric property. Therefore, to find new ways of constructing old curves can be interesting because different machines may recall different mathematical contents: in education that can be useful to foster a unifying vision of different mathematical topics converging toward the same constructed geometrical object.

After the straight line and the circle, the conic sections are possibly the most ordinary shapes that we encounter in our everyday experience: to visualize them, it is sufficient to watch the shadows cast on a wall by tilting a conical lamp-shade. While already studied in the 4th century B.C. by Greek geometers as Menaechmus, the most influent systematic works on conic sections and their properties are referred to Apollonius of Perga around 200 B.C. The same lamp-shade experience embodies the definition of conic sections as the intersection of a circular cone cut by a plane at different inclinations. A conics-drawing device embodying such a definition is the *perfect compass*, known to mathematicians of 17th century but dating back to the 10th-century Arab mathematician Al Quhi ([23], [8]). As visible in Figure 2[1], consider a fixed axis OA and a telescopically-extendable rod OP constrained to keep constant the angle β with the axis. While OP rotates around its axis OA, OP moves on a circular cone. Furthermore, the rod OP can telescopically change its length: by keeping the tracer P in contact with a horizontal plane, the machine plots the intersection of a plane with a circular cone. The trace can be any conic section: introducing the angle α as the inclination of the axis OA with respect to the plane, if $\alpha = \beta$ the result is a parabola, if $\alpha > \beta$ an ellipse (a circumference if $\alpha = \pi/2$), otherwise a hyperbola when $\alpha < \beta$.

While the perfect compass can be used to trace all conic sections, we have many machines designed to trace some specific conics: out of the compass for the circle, there are many tools drawing ellipses, parabolas, and hyperbolas that

[1] Image taken from the page of the site of the Associazione Macchine Matematiche (AMM) `http://www.macchinematematiche.org/index.php?option=com_content&view=article&id=136&Itemid=216&lang=en`, where an explicative animation is also provided.

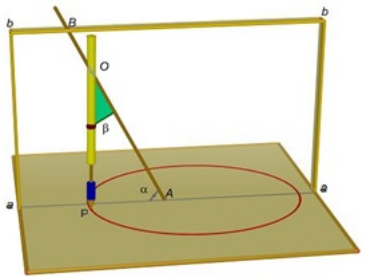

Figure 2: The perfect compass.

have been proposed since antiquity. Examples of these machines can be found in various museums both as original samples, e.g. the National Museum of American History[2], and as reconstructed machines for didactical pathways, e.g. the Associazione Macchine Matematiche (shortly: AMM)[3] of Modena, Italy.

While certain constructions directly embody the definition of the traced curve, e.g. in the gardener's ellipse the thread keeps constant the sum of the distances from the foci, other machines require more attention to be analyzed. In particular, we are going to spend a few words on a class of machines that, adopting straight rods and guides, show the tangent line while tracing the conic. Such machines have in common the use of a deformable rhombus, whose sides can rotate while keeping jointed the final edges.

In the left of Figure 3, we can observe the schema of a machine tracing an ellipse; given the articulated rhombus $ABCD$, the points O and B fixed on the plane constitute the foci of the ellipse, then the intersection P of the straight lines (AC) and (OD) defines an ellipse while D moves along a circle (the director circle of the ellipse relative to the focus O). To prove that P defines an ellipse, i.e. $OP + PB$ is constant, note that $PD = PB$ (the triangles APB and APD are congruent) hence $OP + PB = OP + PD = OD$. Note also that the line (AC), the external bisector of the rays $[PB)$ and $[PO)$, is tangent to the ellipse in P. Indeed, no point Q on (AC) different from P would intersect the ellipse because $OQ + QB > OP + PB$: considering the triangle inequality for OQD, $OQ + QB = OQ + QD > OD = OP + PB$.

Similar reasoning can be applied to all the machines of Figure 3: for hyperbolas, $PA = PC$ because the triangles CPD and APD are congruent, hence $PO - PA = CO$ is constant; for parabolas, $PC = PA$ and (PC) is perpendicular to r. Note that, for the ellipse and the hyperbola, the construction involves the director circle relative to a focus; in the case of the parabola such a circle degenerates in a line, the directrix r (cf. [13]).

These machines not only trace the sought conic, but a rod gives also the direction of the tangent line in the tracing point. Considering the angle limited by the rays linking the point of the curve with its foci, the tangent in the case of

[2] `https://americanhistory.si.edu/collections/object-groups/ellipsographs`
[3] `http://www.macchinematematiche.org/`

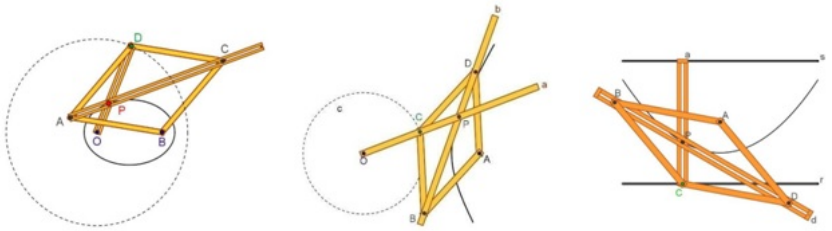

Figure 3: Machines tracing conics by "articulated rhombi:" ellipse (left), hyperbola (centre), parabola (right). Images taken from the AMM's site.

an ellipse is its external bisector, while for the hyperbola is its internal bisector. The parabola has only a finite focus and the other one, according to projective geometry, is a point at infinity that defines the direction of the symmetry axis: in this case the tangent bisects the ray connecting the finite focus and the line passing through the focus at infinity. In Figure 3, the tangent is the external bisector of $[PA)$ and $[Pa)$.

3 Machines for dynamic slope fields

Graphical representations of slope fields involve the simultaneous drawing of directions at many points in the plane. This representation is a static one: by machines we can extend this idea to dynamic slope fields. Indeed, considering a rod r with a point P marked on it, P freely moving on the plane, we could generate a slope field by a mechanism which links the inclination of r to the position of P. Such a variable inclination can be considered to define a slope field over the plane.

This setting is not a static representation of the direction, it is a dynamic instrumental construction of a rod that we can consider as tangent line to the sought curve, thus defining an inverse tangent problem. However, note that we are not yet giving any physical constraint to find orbits starting from an initial value: at the moment we have a dynamic slope field but no means to solve it. One can consider that there are two main classical methods to solve inverse tangent problems, the *approximate* approach and the *analytical* one.

The former constructs approximate solution for the integration of an ordinary differential equation by numerical (finite precision numbers with arithmetic operations) or geometrical (planar constructions with ruler and compass constructions) tools. The Euler method is an example of this approach, the simplest of the Runge-Kutta methods in numerical analysis.

With the *analytical* approach, one formulates the problem with differential equations and tries to solve them rigorously, thereby manipulating it with tools conceptually involving infinite processes, such as limits or series. This approach is the one of classical analysis, from both the more geometrical Newton's idea

of "fluxions and fluents" and Leibniz's more algebraic idea of "infinitesimals."

We are interested in a third way: an *instrumental* approach, the one suggested by the tractional constructions. It allows on the one hand to introduce only finite tools, and on the other hand to obtain an ideally exact solution (not an approximated one, even though subject to physical errors). That can be solved by the introduction of a wheel in P with direction r.

Considering slope fields as the mathematical objects generated by tractional machines (that happens if the analytical counterpart is a first-order ODE), in the following sections 4 and 5 we are going to prove some properties about geometrically generated slope fields (mainly: existence and unicity of solutions). That is necessary to ensure that the machine of section 6 properly works.

4 Two finite foci

4.1 Ellipses

Assuming that we are able to physically pose tangent conditions for a certain conic section, how can we be sure that, fixed an initial point, no other curves share with our sought conic the same tangents? I.e., how can we ensure that the machine solving the generated slope field does not go along any other possible path? An example of a tractional machine with a non-unique path is visible in [19, section 4.1]. In this section we focus on the uniqueness of ellipses: concerning hyperbolas, as well as other isogonal trajectories of confocal ellipses, the uniqueness follows from the results recalled in section 4.2.

Consider two fixed points F_1 and F_2, and let P be a general point in the plane distinct from them. The bisector of the rays $[PF_1)$ and $[PF_2)$ is well defined and so is the exterior bisector, that we assume as tangent direction in P. Considering such tangents for any point on the plane defines a slope field: given these tangent properties, ellipses of foci F_1 and F_2 are solutions of this slope field. We have to prove their uniqueness given an initial point.

Even though it is not strictly necessary, let us introduce a coordinate system such that $F_1(-1,0)$ and $F_2(1,0)$. This will simplify notations and allow us to specify easily some points. Calling $D = \mathbb{R}^2 \backslash \{(-1,0),(1,0)\}$, for any point P in D we consider the anti-clockwise angles $\theta_1(P)$, $\theta_2(P)$ formed by the x-axis and respectively $[F_1P)$ and $[F_2P)$. We are interested in the inclination θ of the external bisector of the rays $[PF_1)$ and $[PF_2)$ with any line parallel to the x-axis. The three angles verify $\theta(P) = \frac{\theta_1(P)+\theta_2(P)+\pi}{2}$.

Note that, while angles can be considered as values in the quotient space $\mathbb{R}/2\pi\mathbb{Z}$, the inclination fits more properly in $\mathbb{R}/\pi\mathbb{Z}$. In these quotient spaces, it is natural to respectively introduce the norms $\|x\|_{\mathbb{R}/2\pi\mathbb{Z}} = \min_{k\in\mathbb{Z}} |x - 2k\pi|$ and $\|x\|_{\mathbb{R}/\pi\mathbb{Z}} = \min_{k\in\mathbb{Z}} |x - k\pi|$.

Let us introduce the following subsets of the plane for a point P in D and an $\epsilon > 0$: we call

$$S_i(P,\epsilon) = \{Q : \|\theta_i(Q) - \theta_i(P)\|_{\mathbb{R}/2\pi\mathbb{Z}} < \epsilon\} \qquad (\text{for } i \in \{1,2\})$$

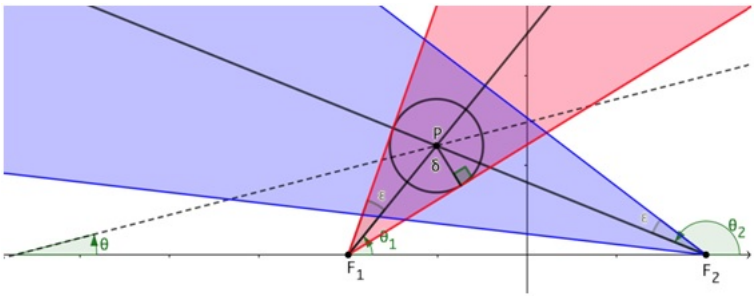

Figure 4: The anti-clockwise angles θ_1, θ_2 and θ are defined by the x-axis (or any parallel line) and, respectively, the rays $[F_1P), [F_2P)$, and the external bisector of $[PF_1)$ and $[PF_2)$ (the dashed line). Given a positive value ϵ, $S_1(P,\epsilon)$ and $S_2(P,\epsilon)$ are respectively the red and the blue area. Considering θ as a direction (i.e. in $\mathbb{R}/\pi\mathbb{Z}$), for all the points Q in $S(P,\epsilon) = S_1(P,\epsilon) \cap S_2(P,\epsilon)$, represented in violet, $\theta(Q)$ has to differ from $\theta(P)$ of less than ϵ. The disk with center P and radius $\delta = \sin\epsilon \cdot \min\{F_1P, F_2P\}$ is a neighbourhood of P included in $S(P,\epsilon)$.

the set of points Q such that the non oriented angle between the rays $[F_iP)$ and $[F_iQ)$ is less than ϵ; consider also $S(P,\epsilon) = S_1(P,\epsilon) \cap S_2(P,\epsilon)$, as represented in Figure 3. To prove the existence and unicity of the solution of a curve of inclination θ let us introduce the following lemma.

Lemma 1. *For any $P \in D, \epsilon > 0$ and $Q \in S(P,\epsilon)$, $\|\theta(Q) - \theta(P)\|_{\mathbb{R}/\pi\mathbb{Z}} < \epsilon$.*

Proof. To prove that the difference of inclination of θ in Q and in P is less than ϵ, we have to start from the definition $S(P,\epsilon) = S_1(P,\epsilon) \cap S_2(P,\epsilon)$. $Q \in S_i(P,\epsilon)$ (with $i \in \{1,2\}$) implies that $\|\theta_i(Q) - \theta_i(P)\|_{\mathbb{R}/2\pi\mathbb{Z}} = \min_{k\in\mathbb{Z}} |\theta_i(Q) - \theta_i(P) - 2k\pi| < \epsilon$. Let k_i be the minimizing integer, therefore $|\theta_i(Q) - \theta_i(P) - 2k_i\pi| < \epsilon$. Since $\theta(Q) - \theta(P) = \frac{\theta_1(Q)+\theta_2(Q)+\pi}{2} - \frac{\theta_1(P)+\theta_2(P)+\pi}{2} = \frac{\theta_1(Q)-\theta_1(P)}{2} + \frac{\theta_2(Q)-\theta_2(P)}{2}$, it follows that $|\theta(Q) - \theta(P) - (k_1+k_2)\pi| < \epsilon$, i.e. $\|\theta(Q) - \theta(P)\|_{\mathbb{R}/\pi\mathbb{Z}} < \epsilon$. □

We can use Lemma 1 to show that $[\theta]_{\mathbb{R}/\pi\mathbb{Z}}$, considered as a function from D to $\mathbb{R}/\pi\mathbb{Z}$, is continuous. For any P in D and any $\epsilon > 0$, by elementary geometric considerations we can observe that, as visible in Figure 4, the open disk centered in P with radius $\delta = \sin\epsilon \cdot \min\{F_1P, F_2P\}$ is included in $S(P,\epsilon)$. Therefore, for every point Q in this disk, $\|\theta(Q) - \theta(P)\|_{\mathbb{R}/\pi\mathbb{Z}} < \epsilon$: that justify the continuity of $[\theta]_{\mathbb{R}/\pi\mathbb{Z}}$.

Now we want to provide two intersecting subsets covering D. L_x is meant to be a set in which θ is quite horizontal, while in L_y θ is quite vertical.

Specifically, fixed any $\epsilon \in]\pi/3, \pi/2[$, we can consider the points $P_1(0, \sqrt(3))$ and $P_2(0, -\sqrt(3))$. Since P_1 and P_2 are on the y-axis, the bisector of their rays is the y-axis and their exterior bisector is parallel to the x-axis, i.e. $[\theta(P_1)]_{\mathbb{R}/\pi\mathbb{Z}} = [\theta(P_2)]_{\mathbb{R}/\pi\mathbb{Z}} = [0]_{\mathbb{R}/\pi\mathbb{Z}}$. Let L_x be $S(P_1,\epsilon) \cup S(P_2,\epsilon)$. By construction, any point

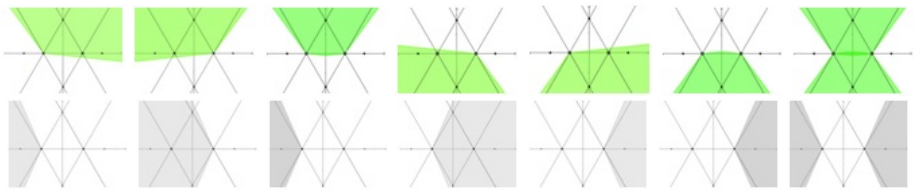

Figure 5: Construction step by step of $L_x = S(P_1, \epsilon) \cup S(P_2, \epsilon)$ and of $L_y = S(P_3, \epsilon) \cup S(P_4, \epsilon)$ given an angle $\epsilon \in]\pi/3, \pi/2[$. Top strip: $S_1(P_1, \epsilon), S_2(P_1, \epsilon), S(P_1, \epsilon), S_1(P_2, \epsilon), S_2(P_2, \epsilon), S(P_2, \epsilon), L_x$. Bottom strip: $S_1(P_3, \epsilon), S_2(P_3, \epsilon), S(P_3, \epsilon), S_1(P_4, \epsilon), S_2(P_4, \epsilon), S(P_4, \epsilon), L_y$.

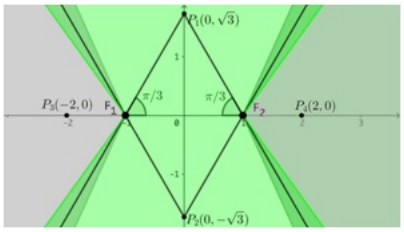

Figure 6: $L_x = S(P_1, \epsilon) \cup S(P_2, \epsilon)$ is the green area (light and dark) and $L_y = S(P_3, \epsilon) \cup S(P_4, \epsilon)$ is the grey and dark green area, given an angle $\epsilon \in]\pi/3, \pi/2[$. Note that $L_x \cup L_y$ covers the whole plane but the foci, and $L_x \cap L_y$, the dark green area, surrounds the rays starting from the foci with an inclination of $\pm\pi/3$.

P in L_x satisfies $\|\theta(P)\|_{\mathbb{R}/\pi\mathbb{Z}} < \epsilon$, thus the inclination is granted not to be vertical ($\epsilon < \pi/2$).

We consider now the points $P_3(-2, 0)$ and $P_4(2, 0)$. Since P_3 and P_4 are on the x-axis externally to F_1F_2, the exterior bisector of their rays has to stay parallel to the y-axis; hence $[\theta(P_3)]_{\mathbb{R}/\pi\mathbb{Z}} = [\theta(P_4)]_{\mathbb{R}/\pi\mathbb{Z}} = [\pi/2]_{\mathbb{R}/\pi\mathbb{Z}}$. Let L_y be $S(P_3, \epsilon) \cup S(P_4, \epsilon)$. By construction, any point P in L_y satisfies $\|\theta(P) - \pi/2\|_{\mathbb{R}/\pi\mathbb{Z}} < \epsilon$, thus the inclination is granted not to be horizontal. The step-by-step construction of L_x and L_y is visible in Figure 5.

Also observing Figure 6, we can easily note that $L_x \cup L_y$ covers D, and that $L_x \cap L_y$ contains a neighbourhood of any point (but the foci) lying on the external rays passing through the foci with a slope of angle $\pm\pi/3$ (these rays are oriented to avoid the strip of the plane with abscissa comprised in $[-1, 1]$).

Hence, the slope field generated by the exterior bisector of $[PF_1)$ and $[PF_2)$ is defined by $dy/dx = \tan\theta$ in L_x and by $dx/dy = \cot\theta$ in L_y. In both L_x and L_y the differential equations are granted to have a unique solution: in these respective domains $\tan\theta$ and $\cot\theta$ are well defined and continuous ($[\theta]_{\mathbb{R}/\pi\mathbb{Z}}$ is continuous). Furthermore, considering the definition of the domains, these functions also have limited slope respectively in L_x and L_y, thus they are Lipshitz continuous (sufficient condition for existence and uniqueness in each domain).

Given an initial point in $L_x \cap L_y$, the unicity on each L_x and L_y ensures unicity on D; given an initial point outside $L_x \cap L_y$, this point belongs necessarily to either L_x or L_y and the unicity of the curve solution there allows to extend it to $L_x \cap L_y$ and finally to the whole D.

Thus the defined slope field has granted the uniqueness of its solutions; since in each point the solution has a tangent orthogonal to the bisector of the rays, which is a characteristic property of ellipses, the only possible traces are ellipses with foci F_1 and F_2.

4.2 Isogonal trajectories of ellipses

Fixed two points F_1 and F_2, the slope field defined by the external bisector of the rays connecting a general point to F_1 and F_2 is solved by all and only confocal ellipses according to the choice of the initial point. To trace the hyperbolas with foci F_1 and F_2, we should consider the internal bisectors instead of the external ones: as already recalled in the tangent properties of section 2, confocal ellipses and hyperbolas intersect orthogonally (however, note that by constructing hyperbolas as slope field trajectories, we can trace only one of the two branches of the curve, the one which goes through the starting point). As a generalization, in 1850 the Italian Gaspare Mainardi [14] posed and solved the problem of determining the oblique trajectories of a system of confocal ellipses (in that sense, the hyperbolas are the *orthogonal trajectories* of the family of confocal ellipses): some examples of such curves are shown in Figure 7[4]. To find out the curves intersecting every member of a given pencil of curves at a constant angle is the problem of isogonal trajectories, a typical problem of differential geometry. Later on, the Indian Sir Asutosh Mukherjee (sometimes anglicized to Mookerjee) remarkably simplified Mainardi's solution by introducing hyperbolic functions [20] (see also [25, pp. 589ff]): the system of curves, cutting a system of confocal ellipses at a constant angle α other than right, is given by

$$x = c\cos(\phi)\cosh(n(\lambda+\phi)), \qquad y = c\sin(\phi)\sinh(n(\lambda+\phi)),$$

where $2c$ is the distance between the foci, n is $\tan\alpha$ and λ is an integrating constant. These symmetrical forms have been included by A. R. Forsyth in his very widespread textbook on differential equations [11, p. 146] as an exercise.

Considering the angle α, by Mukherjee form we can easily evince that isogonal trajectories are transcendental if and only if α is not a multiple of $\pi/2$, i.e. when n is a non-zero real number. Being λ related to the initial value, every trajectory has to be considered while keeping λ constant and varying ϕ. Hence, out of the cases of ellipses and hyperbolas, for $\phi = 2k\pi$ (for any integer k), we can consider the points $(c\cosh(n(\lambda+\phi)), 0)$. Therefore, we have infinite intersections between the curve (that does not contain a straight line) and the

[4]Images obtained using `https://bluffton.edu/homepages/facstaff/nesterd/java/slopefields.html`.

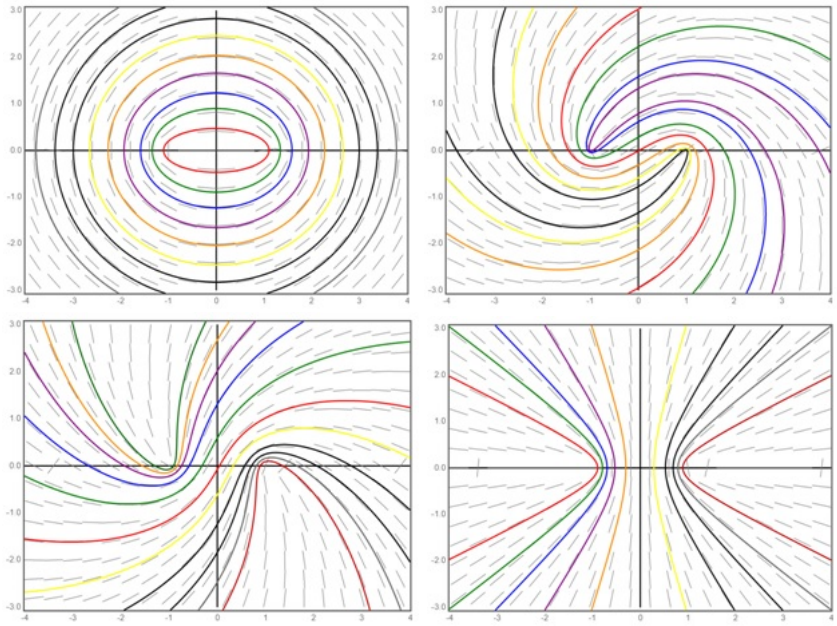

Figure 7: Isogonal trajectories of confocal ellipses (the foci are in $(\pm 1, 0)$) with the angles 0 (ellipses, top left), $\pi/6$ (top right), $\pi/3$ (bottom left), $\pi/2$ (hyperbolas, bottom right).

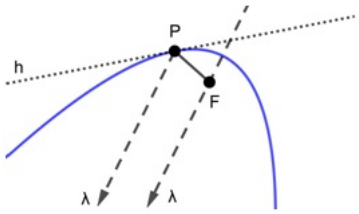

Figure 8: Parabola defined given a finite focus F, an oriented direction λ and passing through a point P. The external bisector h of $[PF)$ and $[P\lambda)$ is tangent to the parabola.

y-axis. For Bézout's theorem, that implies that the solution curves other than ellipses and hyperbolas are transcendental.

To conclude this section let us consider the case $F_1 = F_2$. First of all, the conic degenerate cases are circles (external bisector) or lines (internal bisector). If the two foci coincide, an oblique trajectory has to keep constant the angle between the tangent and the radial direction: therefore the sought curve is a logarithmic spiral, and a machine drawing it behaves as an equiangular compass [18]. From an asymptotic standpoint, far away from the foci, the behaviour of the oblique trajectories is somehow similar to logarithmic spirals even when the two foci do not coincide.

5 One focus at infinity

5.1 Parabolas

In the early 17th century, while conceiving some machines for conical sections, Kepler imagined a machine for the parabola as a machine for the ellipse with a focus at an infinite distance (cf. [10]). We intend to keep this idea and consider parabolas as bifocal conics with one focus at infinity in an oriented direction λ (oriented to define the side in which the parabola opens). Let us underline that, as visible in Figure 8, the tangent at any point P of a parabola with (finite) focus F and oriented direction λ is the exterior bisector of the angle formed by the rays $[PF)$ and $[P\lambda)$, where the latter ray is parallel to and with the same orientation of λ.

Given a fixed point F and an oriented direction λ, parabolas are trajectories of the slope field generated considering as tangent in P the external bisector of $[PF)$ and $[P\lambda)$ but, like for the ellipse in section 4.1, we want to highlight that for every initial point (out of F) the solution is unique. Let us introduce a system of perpendicular coordinates with origin in F and an y-axis s.t. $[Fy) = [F\lambda)$. Consider P and the anti-clockwise angle $\theta_1(P)$ defined by the half-line $[Fx)$ and $[FP)$ (also in this case the angle is defined in the whole plane but F). Note that in this case it is not necessary to consider $\theta_2(P)$ because $[P\lambda)$ is the vertical ray passing through P, thus its slope is constant. Let $\theta(P)$ be the

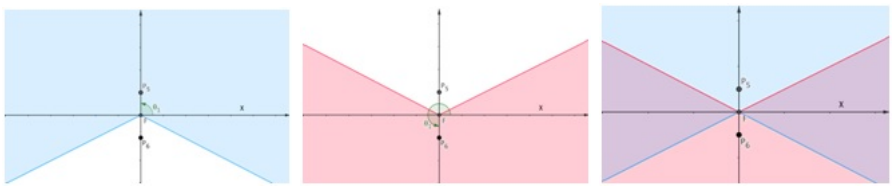

Figure 9: Visualization of $L_y = S_1(P_5, \epsilon)$ [left], $L_x = S_1(P_6, \epsilon)$ [center] and both [right], given an angle $\epsilon \in]\pi/2, \pi[$.

inclination of the external bisector of $[PF)$ and $[P\lambda)$ with any line parallel to the x-axis, hence $\theta(P) = \theta_1(P)/2 + \pi/4$. Let us also introduce $S_1(P, \epsilon) = \{Q : \|\theta_1(P) - \theta_1(Q)\|_{\mathbb{R}/2\pi\mathbb{Z}} < \epsilon\}$. Also in this case we introduce a lemma.

Lemma 2. *For any $P \neq F, \epsilon > 0$ and $Q \in S_1(P, \epsilon)$, $\|\theta(Q) - \theta(P)\|_{\mathbb{R}/\pi\mathbb{Z}} < \epsilon/2$.*

Proof. $Q \in S_1(P, \epsilon)$ implies that exists $k_1 \in \mathbb{Z}$ s.t. $\|\theta_1(Q) - \theta_1(P)\|_{\mathbb{R}/2\pi\mathbb{Z}} = |\theta_1(Q) - \theta_1(P) - 2k_1\pi| < \epsilon$. Since $\theta(Q) - \theta(P) = \frac{\theta_1(Q) - \theta_1(P)}{2}$, it follows that $|\theta(Q) - \theta(P) - k_1\pi| < \epsilon/2$ □

Therefore, for any $\epsilon > 0$, if Q lies in the disk centered in P with radius $\delta = \sin(2\epsilon) \cdot F_1P$, $\|\theta(Q) - \theta(P)\|_{\mathbb{R}/\pi\mathbb{Z}} < \epsilon$; thus $[\theta]_{\mathbb{R}/\pi\mathbb{Z}}$ is continuous in the whole plane but F. To find two intersecting sets covering the domain, fixed any angle $\epsilon \in]\pi/2, \pi[$, consider $P_5(0, 1)$ and $P_6(0, -1)$. As visible in Figure 9, we can introduce $L_y = S_1(P_5, \epsilon)$: $[\theta(P)]_{\mathbb{R}/\pi\mathbb{Z}} = [\pi/2]_{\mathbb{R}/\pi\mathbb{Z}}$ for any point P on the y-axis with positive ordinates and, by Lemma 2, in L_y the inclination θ differs from $\theta(P_5)$ of less then $\epsilon/2 < \pi/2$. Similarly we can consider $L_x = S_1(P_6, \epsilon)$: $[\theta(P)]_{\mathbb{R}/\pi\mathbb{Z}} = [0]_{\mathbb{R}/\pi\mathbb{Z}}$ for any P on the y-axis with negative ordinates and in L_x the inclination θ differs from $\theta(P_6)$ of less then $\pi/2$.

Thus, for continuity and lipshitzianity in intersecting covering sets, we have that the existence and uniqueness of the solution is granted in every point but F. As a degenerate case, the solution starting from a point on the y-axis with positive ordinates coincides with the positive ordinates of the y-axis.

5.2 Isogonal trajectories of parabolas

Given the family of parabolas with the same focus and axis, it is natural to ask ourselves what are the curves intersecting such a family at a constant angle α. Differently from section 4.2, in this case the isogonal curves obtained rotating the exterior bisector of any fixed angle are still parabolas, as we are going to show.

As visible in Figure 10, let us consider the fixed point F and the oriented direction λ. For any point P different from F, by adding an angle α to the exterior bisector h of $[PF)$ and $[P\lambda)$, we obtain the line h_α: that defines a slope field whose solutions are the sought isogonal trajectories. Introducing the direction $\lambda_{2\alpha}$ as λ rotated by an angle 2α, we can prove the following lemma.

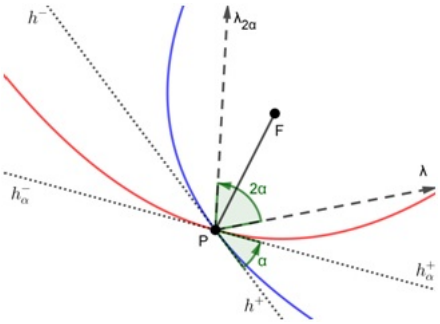

Figure 10: The parabola with focus F and direction $\lambda_{2\alpha}$, i. e. λ rotated of the angle 2α (represented in red) solves the slope field generated by adding an angle α to the exterior bisector h of $[PF)$ and $[P\lambda)$. This curve intersects at an angle α the family of parabolas of focus F and direction λ (in blue we can see such a parabola passing through P).

Lemma 3. *The line h_α is the exterior bisector of $[PF)$ and $[P\lambda_{2\alpha})$.*

Proof. First of all, given a line s passing through a point O, consider its opposite directions s^+ and s^-. Such a line s is the external bisector of $[OA)$ and $[OB)$ if and only if the angle $\widehat{s^+OA}$ is equal to $\widehat{s^-OB}$. Orient h and h_α such that $\widehat{h_\alpha^+PF} = \widehat{h^+PF} - \alpha$, as in Figure 10. Since h is the external bisector of $[PF)$ and $[P\lambda)$, it holds $\widehat{h^+PF} = \widehat{h^-P\lambda}$. For construction $\widehat{h_\alpha^-P\lambda_{2\alpha}} = \widehat{h^-P\lambda_{2\alpha}} + \alpha = (\widehat{h^-P\lambda} - 2\alpha) + \alpha = \widehat{h^-P\lambda} - \alpha = \widehat{h^+PF} - \alpha = \widehat{h_\alpha^+PF}$, hence $\widehat{h_\alpha^-P\lambda_{2\alpha}} = \widehat{h_\alpha^+PF}$, i.e. h_α is the exterior bisector of $[PF)$ and $[P\lambda_{2\alpha})$. □

By this lemma, it follows that the slope field defined by h_α is solved by the parabolas of focus F and direction $\lambda_{2\alpha}$. That means that the isogonal trajectories of the family of confocal parabolas (with finite focus F and oriented direction λ) are yet parabolas.

6 The new machine

6.1 The bisector mechanism

The main aim of this work is to introduce a new machine that draws conics thanks to their tangent properties. Specifically, we need a mechanism for the bisector of the rays connecting the tracing point and the foci (finite or at infinity). A simple mechanism to bisect is shown in Figure 11 (exploded view of the model realized with Autodesk Fusion 360) and in Figure 12 (3D-printed sample). The files necessary to print such a machine are available online at the link `https://www.thingiverse.com/thing:4006566`.

Adopting the notation of Figure 11, the little gear transmits the motion between the top and the bottom gears. Hence, any rotation of the top gear

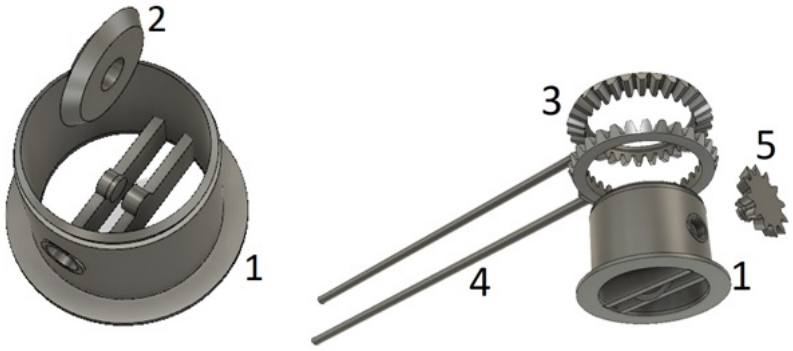

Figure 11: Components of the machine with gears. On the left we can note the wheel (2) that has to be inserted (and constrained to roll) in the central cylinder (1). On the right there is an expanded view of the geared components: the two gears with the rods will stay on the top (3) and on the bottom (4) of the central cylinder (1), and the little gear (5) (fixed on the hole of the central cylinder) will transmit the motion between the top (3) and the bottom (4) gears.

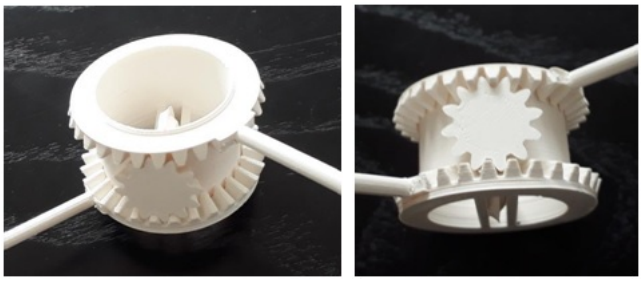

Figure 12: Main mechanism: the bisector (eventually added by a constant angle) is obtained thanks to three conical gears. The position of the little conical gear gives the direction of the wheel that touches the plane.

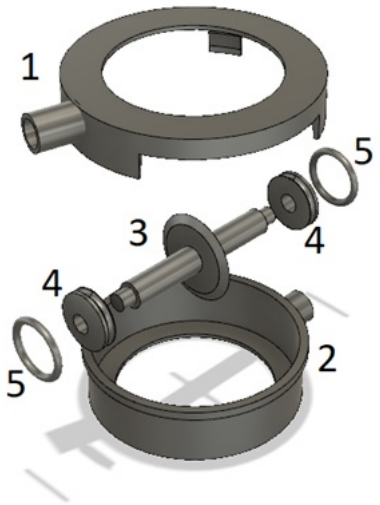

Figure 13: Components of the bisector mechanism with tyres. The rods (not shown in the image) have to be inserted in the holes of the top (1) and bottom (2) components. Note that a click mechanism allow them to rotate (the top will be external to the bottom component) while keeping the wheeled-axis (3) inside. Furthermore, two little pieces (4) are necessary to hold the O-rings (5): while the top and the bottom components are kept together by the click mechanism, the pressure grants (with a certain degree of precision) that the O-rings roll without slipping on the horizontal parts of (1) and (2).

around the central cylinder causes a symmetric rotation of the bottom one with respect to the plane of the wheel. To deepen this behavior, we name the mechanism to be in the "0-position" when the rods are parallel, one above the other (like lancets of a clock at noon).

If in the 0-position the rods lie on the plane of the wheel, also when they turn around the central cylinder the wheel direction is always constrained to be the bisector of the rods. Similarly, if in the 0-position the plane of the wheel defines an angle α with the rods, also when the rods rotate the direction of the wheel is the bisector rotated by α . Trivially, for the external bisector we can consider $\alpha = \pi/2$.

Note that, differently from machines as the spirograph, in our machine the number of teeth is not important: the bisector can also be implemented by two flat cylinders whose rotation is transmitted by rubber wheels, as visible in Figure 13 and Figure 14 (however, that implies problems related to possible slipping). Such a 3D model is available at `https://www.thingiverse.com/thing:4006702`.

Fixed the passage of the rods through the foci (aim of the next section), the wheel gives the direction of the tangent that the curve-to-be has to satisfy.

Figure 14: A bisector machine using rubber wheels to avoid gears. The two rubber wheels share the same axis, but they can rotate independently.

Hence, suitably adopted, our mechanism can be part of a machine drawing conics and oblique trajectories. Actually, taking into account the huge difference between machines posing direction-properties and position-properties (recalling section 1, non-holonomic vs holonomic constraints), differently from the machines of section 2 the practical use of our mechanism requires a certain attention to the composition of the substrate. Indeed, to improve the resistance to lateral forces and, in the meanwhile, to make the wheel easily mark its path, we suggest the adoption of a foam sheet. On it, the curve appears as a furrow carved out by the wheel.

6.2 Passage through the foci

We introduced the bisector mechanism to pose the tangent condition, but to trace our sought curves we still need to constrain a rod to pass through a focus (both finite and at infinity). To make a rod projection pass through a finite focus we could use a vertical peg with a horizontal hole. If the peg can rotate around its center (e.g. by a pin) in a point F of the plane, the passage of the rod through the hole ensures that the projection of the rod on the plane has to pass through F. To pin the physical peg on the plane, we should put a base in cork, softwood or thick cardboard below the foam sheet. However, even to trace an ellipse, to constrain foci by cylinders with holes would imply problems (assuming the rods moving at different heights, while rotating the lowest rod can collide with the peg of the other rod). Thus, to trace conics without rod/peg collisions, we propose a solution allowing rods to switch foci when they are superimposed. This solution is possible by the pegs visible in Figure 15.

The peg has two carvings: each of them allows the rod at its height to enter and exit only from one side. Seen from above, the upper carving opens in the opposite direction of the lower one. To allow a simple visualization, we indicate the direction in which the rod can come in the carving by an arrow. To distinguish between the uppest and the lowest level (both for rods and carvings), we color the first by blue and the latter by red. Figure 16 shows how the switching works out, allowing to trace whole ellipses (in this case the switch repeats every

Figure 15: Left: model of a peg for a finite focus. Center: a 3D printed peg, including inside a drawing pin (glued in the bottom hollow). Right: bisector mechanism with two pegs constraining the passage of the rods.

time the tracing point is aligned with the foci). While such pegs permit to continually trace conics, such an idea does not solve in general the problem of rod/peg collision for general isogonal curves, as visible in Figure 17.

Recalling section 5, to draw parabolas the "focus at infinity" condition implies that one of the two rods has to translate. That can be easily implemented by a hollowed cylinder that rotates without slipping on the plane while rotating and sliding along the section of a rod. The Figure 18 shows how to use a 3D printed cylinder around the rod that has to pass through a focus at infinity.

We can note that even the drawing of the parabola can be afflicted by problems due to the collision between the translating rod and the peg. That can be avoided if we adopt as direction of the wheel the internal bisector: according to the notation of section 5, in this case the ray $[P\lambda)$ will meet the focus F in no configuration.

As a final remark, we can note that, if we have as foci two points at infinity, it is like having two cylinders keeping the rods moving in a parallel way. In this case, untreatable by our components because we provide a cylinder only for the lowest rod, the angle of the wheel would be constant and the traced curve would be a straight line.

Once introduced how to set the passage through the foci, we can finally consider how to use the machine to trace a trajectory.

6.3 Operating instructions

Before using the machine to trace a curve, we have to suitably set some parameters to make the machine solve a specific slope field. Curves traceable by our machine are defined by three settings:

1. the angle between the bisector of the rods and the direction of the wheel;
2. the foci;
3. the starting point.

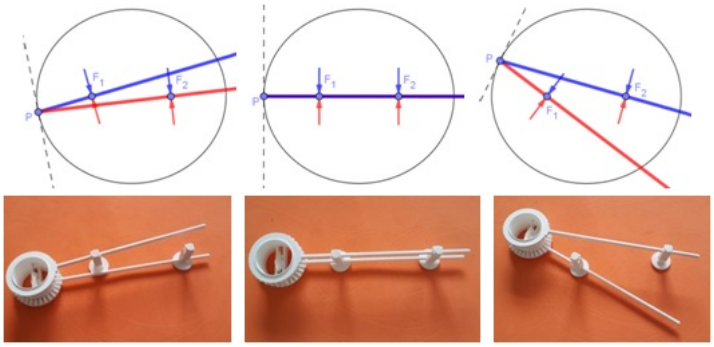

Figure 16: If properly set, with such pegs it is possible to trace continuously an ellipse. In this sequence of images (top: simulations, bottom: photos): while the wheel moves upward, rods switch their foci. In the first step the uppest blue rod passes through F_1 and the lowest red one through F_2: in the third step the rods inverted their foci. The switching is possible because the rods of a certain color (i.e. at a certain height) arrive/depart from the foci according to the direction of the arrow of the same color (i.e. with the right direction of the carving at their own height). That can be summarized by the condition that carvings have to be external to $\widehat{F_1PF_2}$ (both the blue arrow on the blue rod and the red arrow on the red rod have to be external to the angle $\widehat{F_1PF_2}$).

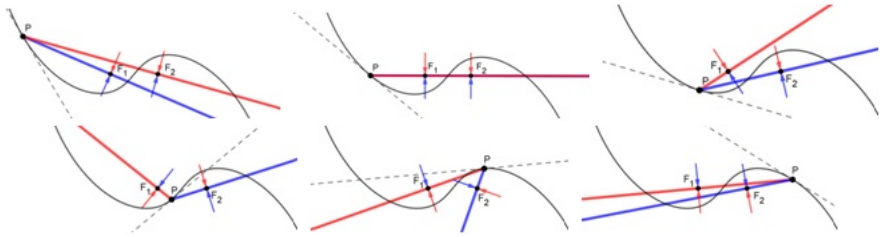

Figure 17: Even though such pegs permit the continuous drawing of conics, some paths cannot be continuously traced. Following the shown motion along an isogonal to confocal ellipses (curve obtained by posing the parameters $c = 1, \lambda = \pi/2, n = -1.2$ in Mukherjee's formula of section 4.2), rods can switch the first time they overlap (second step), but not the second time (last step). Indeed, in the last image, the red rod meets the blue arrow in F_2 and vice-versa for the blue rod on F_1, thus rods can no longer change their foci and collide with the pegs. According to the end of the caption of Figure 16, in this case the problem arises when P passes between the foci (steps 4, 5), when the carvings pass from external to internal to $\widehat{F_1PF_2}$.

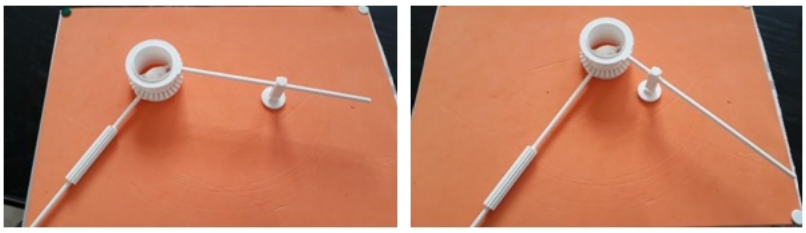

Figure 18: A cylinder that rotates without sliding on the plane can impose the translation of a rod to trace parabolas. To avoid sliding, the external part of the cylinder isn't smooth but has many long thin teeth.

The first parameter can be easily set by superimposing the rods, i.e. putting them in 0-position (cf. section 6.1). More precisely, we can follow the following steps:

- the little gear is taken away, leaving the two geared rods free to rotate around the central cylinder;
- the rods are brought to the 0-position by rotating top and bottom gears;
- the cylinder is rotated up to defining the desired angle between the superposed rods and the wheel direction;
- the little gear is put back on the cylinder lateral hole to keep constant the angle between the bisector of the rods and the direction of the wheel.

To set foci we have to distinguish two cases. For a finite focus we pin a peg of Figure 15 on the plane, while for a focus at infinity we put the cylinder of Figure 18 around the lowest rod. If the two foci are both finite, we have to take care of putting the rods in the carving at their heights and, according to the caption of Figure 16, carvings have to be external to the angle defined by the two rods to allow them to switch pegs. If a focus is at infinity, we have to put the cylinder on the plane in the desired direction.

Let us summarize all the possibilities: with two pegs, when the wheel and the bisector of the rods are aligned up, the upcoming curve is a hyperbola; when wheel and bisector are perpendicular, it is an ellipse; with any other angle between wheel and bisector, the curve is one of the isogonal trajectories of ellipses (section 4.2). With one peg and the hollowed cylinder, the curve is always a parabola.

Finally, to choose the initial point, we simply put the wheel on a specific point of the foam sheet. This selects one trajectory in the slope field defined by the first two settings (angle and foci).

Once set the machine, to produce the plot we still have to take care of several things. Without preventing the rotation of the top gear, the user must push the top of the cylinder both vertically (to press the wheel on the foam sheet) and horizontally (to make the wheel move forward). While moving, the rods

must be kept inside the pegs (or, in the case of a focus at infinity, we have to rotate the teethed cylinder on the plane avoiding its slipping). These conditions ensure the uniqueness of the motion. Finally, the expected curve appears as a furrow in the foam sheet.

7 Educational fallouts

Out of introducing a new machine for conics and their isogonal curves, the aim of this paper is to give the chance to everyone to easily (and cheaply) get its own machine: that seems particularly interesting for educational purposes. The use of tractional machines in education is new in today mathematical education, even though we can imagine that it was already adopted in Italy by Giovanni Poleni in Padua (first half of the 18th century) and Ernesto Pascal in Naples (beginning of the 20th century). About Poleni, he was the first who proposed the machines for the tractrix and the logarithmic curve [21] that were also built and used in his cabinet of experimental philosophy for exhibitions and probably in teaching.

Today, many (non-tractional) curve-drawing machines have been transposed in the classroom for laboratory activities (e.g. [1], [15]), with also interests from a historical and epistemological perspective. Indeed, since motion and manipulation are not so widely adopted in classroom teaching, the exploration of curve-tracing machines can offer interesting unusual standpoints to the curricular mathematical contents. According to the framework of the theory of *semiotic mediation* [2], a fruitful exploration of a machine should start from a physical manipulation and then move to a conceptual and mathematical understanding of the artefact. The underlying cognitive theory is the *embodiment*, i.e. the idea that the human understanding is shaped by aspects of the whole body and not solely by the use of language and formalism [26], [22]. The didactical use of mathematical machines also overcomes the boundaries of pure mathematics, and interests intersections with fields as art or architecture [9].

About our machine, we think that it could be proposed with different purposes at different levels: to high-school and university students, to math teachers, to professional mathematicians. According to the level, the exploration of the machine can also naturally lead to deepening other related topics. For example, in physics the properties of tangents to conics [7] offers a rich connection to light reflection on parabolic or elliptical mirrors, parabolic antennas and concentrator mirrors. In projective geometry one could deepen the role of the passage from finite foci to points at infinity, passing from the affine to the projective plane.

As evinced by the only (at our knowledge) experimental paper on tractional machines [16], with a complex machine it is not so spontaneous to focus on the role played by the wheel to trace a curve given its tangent properties. Therefore, to foster the attention on the main components, we think that for some activities it could be more appropriate to start from a simplified tractional machine tracing

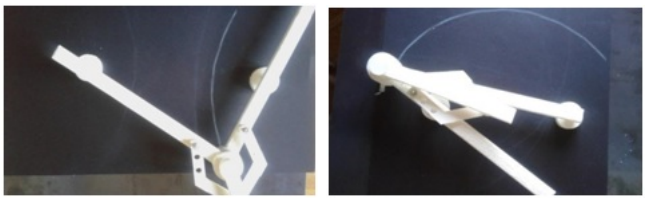

Figure 19: Simplified machine tracing a hyperbola (left) and an ellipse (right).

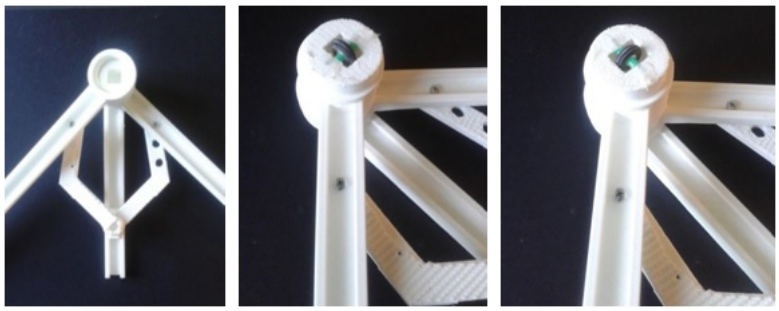

Figure 20: The simplified machine seen from below. Left: the mechanism for the bisector without the wheel (the little rods are not straight to permit a larger opening). In the other pictures, the wheel is put to trace a hyperbola (center) and an ellipse (right).

only ellipses and hyperbolas (see Figure 19 for the traced curves and Figure 20 to deepen the mechanism: downloadable files are available online at `https://www.thingiverse.com/thing:4012950`). Specifically, by constructing the bisector by linkages (without gears), this machine embodies the beautiful property of constructing curved lines starting only from straight components, in the same spirit as the articulated-rhombus machines of section 2. Differently from the other proposed machine, this one requires also hardware out of 3D printed components (a metal base, magnets for the pins, sandpaper for the base of the pins, screws and nuts, a toy-car wheel, a steel pin as axis, a spring and a chalk to put the white pigments on the rubber of the wheel). The reader interested in the details of the construction can contact us for further information.

8 Conclusions

In this paper, we introduced a new device to trace all the conics using the property of their tangents according to the position of the foci (on the plane or at infinity). Furthermore, the device can also trace transcendental curves (isogonal trajectories of confocal conics): such a property should have been considered really weird by 17th-century mathematicians soon after the spread of Cartesian geometry and the related dualism between algebraic and transcendental curves.

However, such behaviour is not new: the more recent example is probably a tractional machine introduced in [24] and explored in [16] which, by the change of direction of a right angle, traces a parabola or an exponential. However, the first and more extraordinary example of a problem in which a variation in parameters cause algebraic or transcendental curves is the late 17th-century "Bernoulli's problem" [4, pp. 32-43]. This is a generalization of the tractrix: on the x-axis consider the endpoint of a cord $(t, 0)$ whose length varies proportionally to t, let's say pt (where p is a constant). If the other endpoint of the cord imposes the tangent condition pointing to $(t, 0)$, we have that for rational values of p the curve is algebraic (if $p = 1$ we construct circular arcs), otherwise the solution is transcendental. A machine for such a problem was sketched by Jakob Bernoulli.

To conclude, we hope that this work could provide a technical basis for the widespread of tractional machines (the 3D printable files are freely available on the site `https://www.thingiverse.com/`) in order to make students perceive more concretely some mathematical contents usually considered useful but abstract. As a motto, the aim is to touch the transcendence.

Acknowledgement

We are grateful to Davide Crippa and Franco Ghione for historical references. We also thank the UBO-OpenFactory of Brest `https://uboopenfactory.univ-brest.fr/` (especially Laurent Marchal), the secondary school Montessori-Da Vinci and the Fondazione Carisbo of Porretta Terme for the use of their 3D-printer laboratories.

References

[1] Bartolini Bussi, M. G. & Maschietto, M. (2006). *Macchine matematiche. Dalla storia alla scuola*. Springer

[2] Bartolini Bussi, M. G. & Mariotti, M. A. (2008). Semiotic mediation in the mathematics classroom: artifact and signs after a Vygotskian perspective. In English e al. (Eds.) *Handbook of International Research in Mathematics Education* (pp. 746-783). New York and London, Routlegde

[3] Blasjo, V. (2017). *Transcendental Curves in the Leibnizian Calculus*. Academic Press.

[4] Bos, H. J. (1988). Tractional motion and the legitimation of transcendental curves. *Centaurus*, 31(1), 9-62.

[5] Bos, H. J. (2001). *Redefining Geometrical Exactness: Descartes' Transformation of the Early Modern Concept of Construction*. Springer Science & Business Media.

[6] Crippa, D. & Milici, P. (2019). A Relationship between the Tractrix and Logarithmic Curves with Mechanical Applications, *The Mathematical Intelligencer*, 41(4), 29-34, DOI 10.1007/s00283-019-09895-7.

[7] Courant, R. & Robbins, H. (1941). *What Is Mathematics?*, Oxford University Press

[8] De Vittori, T. (2011). The perfect compass: conics, movement and mathematics around the 10th century. In Barbin, E., Kronfellner, M and Tzanakis, C. (Eds) *History and epistemology in mathematics education. Proceedings of the 6th European Summer University*, Vienna, Austria. pp.539-548. `http://numerisation.univ-irem.fr/ACF/ACF11006/ACF11006.pdf`

[9] Farroni, L. & Magrone, P. (2016). A Multidisciplinary Approach to Teaching Mathematics and Architectural Representation: Historical Drawing Machines. Relations Between Mathematics and Drawing. *Proceedings of the 2016 ICME Satellite Meeting of the International Study Group on the Relations Between the History and Pedagogy of Mathematics*. L. Radford, F. Furinghetti, T. Hausberger eds. Montpellier, IREM de Montpellier, pp. 641-651.

[10] Ferrara, F. & Maschietto, M. (2013). Are mathematics students thinking as Kepler? Conics and mathematical machines. In *Eight Congress of European Research in Mathematics Education (CERME8)*. Ankara, Turkey: Middle East Technical University and ERME, pp. 635-644.

[11] Forsyth, A. R. (1948). *A treatise on differential equations*, reprinted 1929 6th ed., MacMillan & co., London. `https://archive.org/details/ATreatiseOnDifferentialEquations_650`

[12] Kempe, A. B. (1876). On a general method of describing plane curves of the n th degree by linkwork. *Proc. London Math. Soc.*, 7, 213–216.

[13] Lebossé, C. & Hémery, C. (1961). *Géométrie*. Gabay, Paris.

[14] Mainardi G. (1850). Sulla integrazione delle equazioni differenziali, *Annali di Scienze Matematiche e Fisiche*, 1, 50-89, 251-255.

[15] Maschietto, M. & Bartolini Bussi, M. G. (2011). Mathematical machines: from history to mathematics classroom. In *Constructing knowledge for teaching secondary mathematics* (pp. 227-245). Springer, Boston, MA.

[16] Maschietto, M., Milici, P. & Tournès, D. (2019) Semiotic potential of a tractional machine: a first analysis, In: U. T. Jankvist, M. van den Heuvel-Panhuizen, & M. Veldhuis (Eds.), *Proceedings of the Eleventh Congress of the European Society for Research in Mathematics Education (CERME11)*, Utrecht, the Netherlands: Freudenthal Group & Freudenthal Institute, Utrecht University and ERME, pp. 2133-2140.

[17] Milici, P. (2012) Tractional motion machines extend GPAC-generable functions. *International Journal of Unconventional Computing*, 8:3, 221-233.

[18] Milici, P. & Dawson, R. (2012), The Equiangular Compass, *The Mathematical Intelligencer*, 34(4), 63–67, DOI: 10.1007/s00283-012-9308-x.

[19] Milici, P. (2020). A differential extension of Descartes' foundational approach: A new balance between symbolic and analog computation, *Computability*, 9(1) , pp. 51-83, DOI: 10.3233/COM-180208

[20] Mookerjee, A. (1887). On the differential equations of a trajectory, *J. Asiat. Soc. Bengal*, 56.2.1, 117–120.

[21] Poleni, G. (1729). *Epistolarum mathematicarum fasciculus*. Patavii: Typographia Seminarii.

[22] Radford L., Bardini C., Sabena C., Diallo P. & Simbagoye A. (2005). On embodiment, artifacts and signs: a semiotic-cultural perspective on mathematical thinking, in Chick H.L. & Vincent J.L. (eds.). *Proceedings of the 29 Conference of the international group for the psychology of mathematics education (PME 28)*, Vol.4, pp. 73- 80, Norway: Bergen University College

[23] Rashed, R. (1990). A Pioneer in Anaclastics: Ibn Sahl on Burning Mirrors and Lenses, *Isis*, Vol. 81, No. 3, pp. 464-491, The University of Chicago Press on behalf of The History of Science Society

[24] Salvi, M. & Milici, P. (2013). Laboratorio di matematica in classe: due nuove macchine per problemi nel continuo e nel discreto, *Quaderni di Ricerca in Didattica (Mathematics)*, 23, 15-24.

[25] Sar, S. (2015). Asutosh Mukhopadhyay and his mathematical legacy. *Resonance*, 20(7), 575-604.

[26] Tall, D. (2013), *How Humans Learn to Think Mathematically: Exploring the Three Worlds of Mathematics*, Cambridge University Press

[27] Tournès, D. (2009), *La construction tractionnelle des équations différentielles*, Paris: Blanchard, 2009.